Geofísica Internacional (2025) **64-3**: 1677 - 1689

Prediction of permeability and effective porosity values using ANN in Maleh field

Mohammed Essa Nassani[1] and Ali Alaji[2]

Abstract

This study presents the development of an intelligent system designed to predict permeability and effective porosity in wells where core samples are unavailable. An artificial neural network (ANN) was constructed with three hidden layers—comprising 15, 10, and 4 neurons, respectively—utilizing well logging parameters (CAL, VCL, NPHI, RHOB, DT) as inputs. The ANN outputs predicted permeability and effective porosity values with remarkable accuracy. The network was optimized with a learning rate of 0.05, a momentum coefficient of 0.95, and the LOGSIG activation function, applied across layers. Input values were normalized to the range of 0 to 1, and training was performed using the sequential forward backpropagation algorithm (newcf). The training phase achieved a minimum mean square error of 0.00001 within 58 seconds over 12,000 cycles, delivering a 100% recognition rate for the training data. The ANN was tested on independent data and demonstrated exceptional performance, achieving 96% accuracy for effective porosity and 98% for permeability predictions in sandstone formations. This efficient algorithm eliminates the need for core sample analysis, reducing costs and time while improving prediction reliability, making it a valuable tool for subsurface characterization and resource exploration.

Key words: Maleh Field, well logging, Permeability, effective porosity, artificial intelligence, Cores, Artificial Neural Network (ANN).

Resumen

Este estudio presenta el desarrollo de un sistema inteligente diseñado para predecir la permeabilidad y la porosidad efectiva en pozos donde no se dispone de muestras de núcleo. Se construyó una red neuronal artificial (ANN) con tres capas ocultas, que consisten en 15, 10 y 4 neuronas, respectivamente, utilizando parámetros de registro de pozos (CAL, VCL, NPHI, RHOB, DT) como entradas. La ANN genera valores predichos de permeabilidad y porosidad efectiva con una precisión notable. La red se optimizó con una tasa de aprendizaje de 0.05, un coeficiente de momento de 0.95 y la función de activación LOGSIG aplicada en las capas. Los valores de entrada se normalizaron en un rango de 0 a 1, y el entrenamiento se realizó utilizando el algoritmo de retropropagación secuencial (newcf). La fase de entrenamiento logró un error cuadrático medio mínimo de 0.00001 en 58 segundos durante 12,000 ciclos, alcanzando una tasa de reconocimiento del 100% en los datos de entrenamiento. La ANN se probó con datos independientes y mostró un rendimiento excepcional, logrando una precisión del 96% para las predicciones de porosidad efectiva y del 98% para las estimaciones de permeabilidad en formaciones de arenisca. Este algoritmo eficiente elimina la necesidad de análisis de muestras de núcleo, reduce los costos y el tiempo, y mejora la fiabilidad de las predicciones, convirtiéndose en una herramienta valiosa para la caracterización del subsuelo y la exploración de recursos.

Palabras clave: Campo Maleh, registro de pozos, permeabilidad, porosidad, inteligencia artificial, núcleos, red neuronal artificial (ANN).

Received: 23 October, 2024; Accepted: June 7, 2025; Published on-line: July 1, 2025.

Editorial responsibility: Dr. Leonid Sheremetov

* Corresponding author: Mohammed Essa Nassani, essanassani@gmail.com
[1] Damascus University, Faculty of Science, Department of Geology, PhD Student, Damascus, Syrian Arab Republic.
[2] Damascus University, Faculty of Science, Department of Geology, Associate Professor, Syrian Arab Republic.

Mohammed Essa Nassani, Ali Alaji

https://doi.org/10.22201/igeof.2954436xe.2025.64.3.1830

1. Introduction

Our study employed data from the Maleh field, situated in the Euphrates Basin in eastern Syria (Figure 1), the Post Judea Sandstones (PJS) is main reservoir, where 51 boreholes were drilled. We utilized a trainable sequential forward backpropagation neural network (newcf) with three hidden layers: the first layer comprising 15 neurons, the second layer 10 neurons, and the third layer 4 neurons. The inputs to the network included well logging parameters (CAL, VCL, NPHI, RHOB, DT). The output of the artificial neural network represents the predicted permeability and effective porosity values. Advanced software programs such as IP-2018 and MATLAB were utilized to achieve the objectives of this study.

This study aims to predict the permeability and effective porosity of wells lacking core samples by utilizing an artificial neural network (ANN) based on well logging and laboratory measurements from cores within the study area. Reservoir characterization plays a pivotal role in determining the economic viability of reservoir development. However, this process is inherently complex due to the heterogeneous nature of most reservoirs, which arises from their depositional environments and the physical characteristics of the rock.

Porosity and permeability are essential parameters for evaluating both the volumetric capacity and flow behavior of reservoirs. While porosity can be estimated more straightforwardly from well logs, permeability remains particularly challenging to determine due to its dynamic nature. Consequently, numerous methods have been developed to improve permeability predictions.

Chehrazi *et al.* (2012) proposed a comprehensive study for predicting permeability using both theoretical and computational models. In their theoretical model, porosity and initial water saturation served as input parameters. Sultan *et al.* (2013) employed a backpropagation neural network to estimate permeability values in the Hanping gas field in northeastern Bangladesh. They divided their dataset into two groups: 74.2% of the total samples were used to train the model, while the remainder was reserved for testing. The neural network demonstrated robust performance, achieving a correlation coefficient of $R = 0.81$. However, a significant limitation of this model was the difficulty in obtaining permeability data from laboratory-measured core samples.

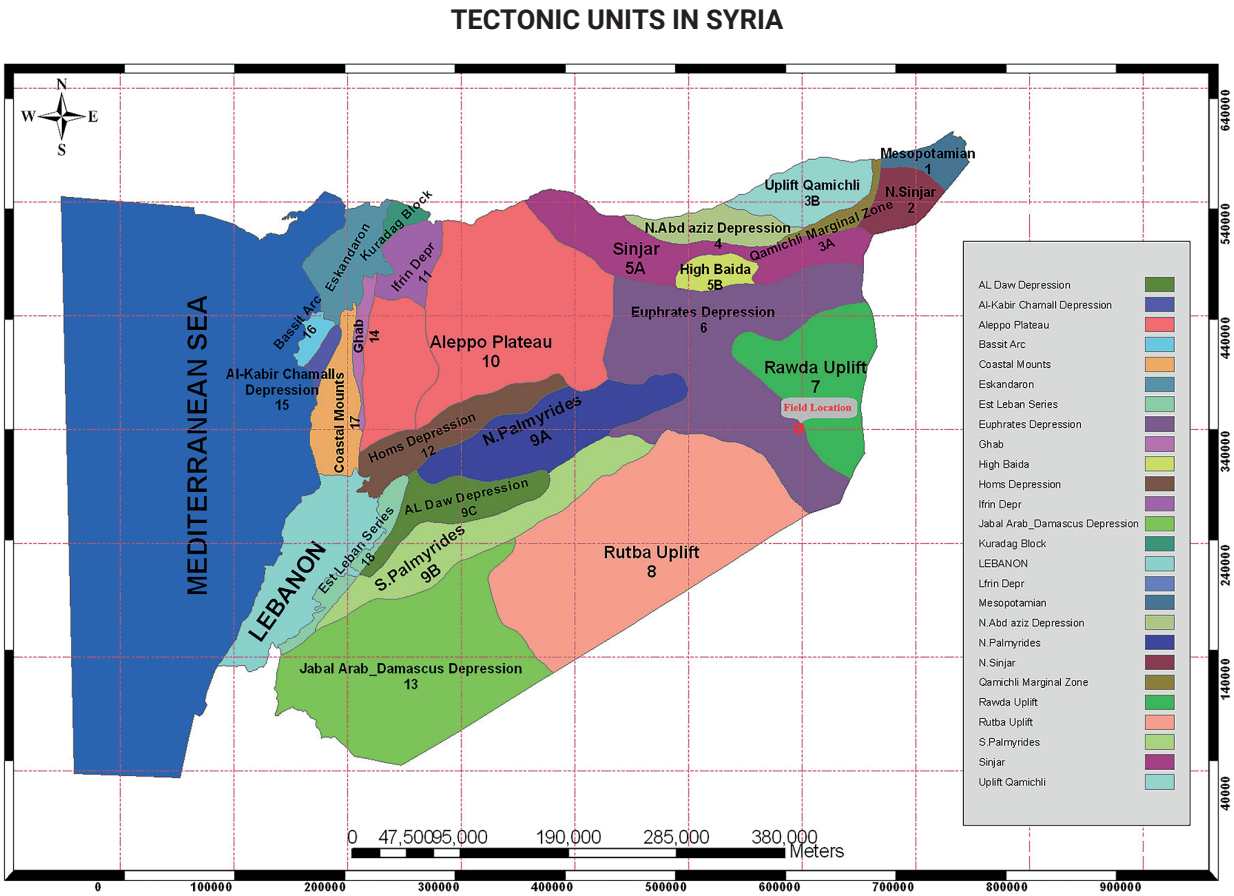

Figure 1. Maleh oil field location

Helle *et al.* (2002) and Lim *et al.* (2004) emphasized the widespread use of well log interpretations for estimating porosity and permeability at various depths. This approach is favored due to its relatively lower cost compared to coring and its ability to compensate for the lack of continuous data from core samples. Furthermore, Lucia *et al.* (2013) highlighted that petrophysical heterogeneity is prevalent in carbonate reservoirs. This heterogeneity is evident in the significant variation of porosity-permeability cross plots derived from core analyses. Research indicates that basic rock fabric controls this variability, with porosity and permeability exhibiting minimal spatial correlation and substantial variability at small scales (inches to feet).

Rock typing is one of the most critical tools for predicting unknown reservoir properties, particularly permeability in un-cored intervals (Fadhil *et al.* 2020; Lis-Sledziona, 2019). While core samples are vital for obtaining fundamental data, coring all wells in extensive fields or all zones of interest within a single well imposes significant financial constraints. Empirical relationships between core-measured porosity and permeability can also be employed to estimate permeability in such scenarios.

Smith *et al.* (1999) proposed a neural network algorithm for predicting porosity, permeability, and grain density using gamma-ray, neutron porosity, and sonic travel time as inputs. Their predicted petrophysical properties closely matched core data, and errors were evaluated within predefined tolerances.

Khayer *et al.* (2022) introduced an efficient method for seismic attribute estimation through image segmentation using a logistic function. Their ANN model revealed a complex relationship between rock properties and wireline data. Additionally, Rezaee *et al.* (2012) and Anifowose *et al.* (2013) developed ANN models using the backpropagation algorithm to predict porosity through both genetic and non-genetic approaches. These models incorporated multiple inputs to design ANN structures suited for their applications.

In the realm of advanced algorithms, Zhong *et al.* (2019) explored convolutional neural networks (CNNs) for predicting various well logs. Despite their ability to handle intricate relationships, CNNs require extensive training data and are computationally slower than ANN models. Challenges such as overfitting, exploding gradients, and class imbalance further complicate CNN training.

Zhang *et al.* (2018) proposed a cascaded long short-term memory (C-LSTM) approach based on the LSTM framework. Although LSTM-based models can generate well logs, their predictive accuracy remains limited when training datasets are small. To address this, Chen *et al.* (2019) introduced an ensemble neural network (ENN) approach. While ENNs are advantageous for small datasets, they are less effective for sequential data.

2. Regional setting

The Maleh Field is part of the Tanak Area and is approximately 13 km north east of the Tanak CPF. The field currently has 45 producing wells, of which 8 simple horizontals and 2 multi-lateral horizontal sidetracks, and 6 injection wells.

2.1 Geology

The Euphrates depression is located above the slope structures of the Arabian plate, with its fixed and mobile sections, and is filled with large thicknesses of marine and continental Neogene sediments. The layers are arranged almost horizontally, with a slope of no more than 3 to 4 degrees. The thickness of the sedimentary cover reaches several kilometers, and dates back from the Ordovician to the Miocene age, and includes several hydrocarbon reservoir formations, which gives it great importance from an economic point of view (Litak *et al.*, 1998). The field has an expectation STOIIP of 333 MMstb mainly in the Post Judea Sandstones (PJS).

2.2 Structure

The throw of the faults varies according to the tectonic activity to which they are exposed (De Ruiter *et al.*, 1995), so that they form a ladder structure on both sides of the river, as Figure 2 shows the ladder structure of the faults of the Euphrates Basin. The depth of the depression increases in the northwest direction, i.e. away from the Rawdah and Rutbah rises. The Euphrates depression consists of a group of blocks separated from each other by normal faults (northwest-southeast) with large throws as in the southeastern section. These blocks do not lean towards the center of the depression but away from it, while in the northeastern section they lean towards the axis of the central depression, and are characterized by their narrowness and great depth.

The Maleh field is a faulted dip-closure at base seal (top Derro – top PJS) level. Base seal is recognized to be the lower part of the Ramah formation. The southern part of the field is intensely faulted. This area displays a number of down stepping and south dipping faulted terraces/blocks.

3. Methodology

MATLAB-2022a was utilized in this study to predict effective porosity and permeability values in wells without core samples. The algorithm development encompassed several stages: training, testing, and generalization.

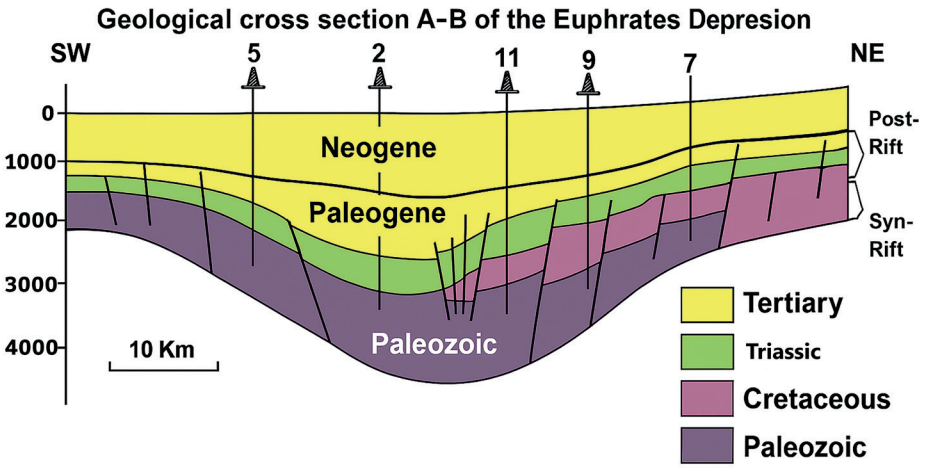

Figure 2. Geological cross section A-B of the Euphrates Depression from SW to NE (De Ruiter *et al.*, 1995).

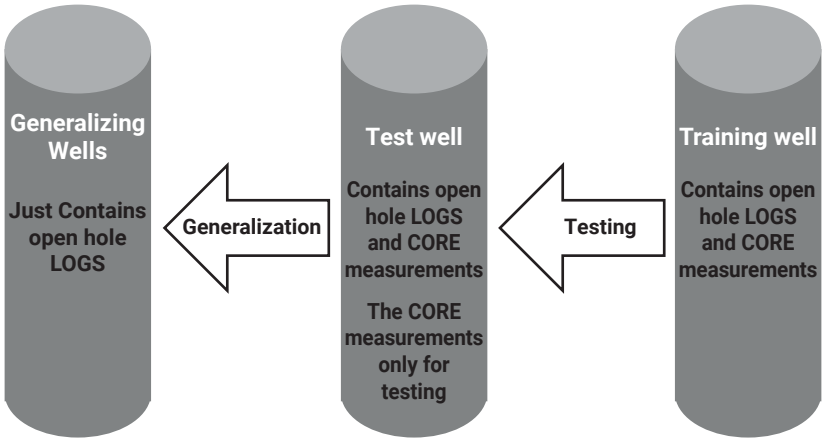

Figure 3. Work stages until reaching the network generalization.

3.1 Data extraction stage:

Core measurements were carried out on three wells, namely: MAL-102, MAL-107 and MAL-111.

The available samples were divided into two groups: the first group was used in the network training process, while the second group was used to test the network results. The training data consisted of 65% of the total output data, which served as the target for the values predicted using the neural network. The testing data comprised the remaining 35%. MAL-102 and MAL-111 wells were selected as training wells, while the MAL-107 well was selected for testing. Additionally, MAL-103 and MAL-115 wells were chosen to demonstrate ANN generalization.

3.2. Preparing the database

The input dataset is organized into TXT files, with the first column representing depth, the second column indicating the volume of clay (VCL), Where VCL was calculated scientifically by GR log using the following equation:

$$\mathrm{IGR} = \mathrm{Vsh} = \frac{\mathrm{GRlog} - \mathrm{GRmin}}{\mathrm{GRmax} - \mathrm{GRmin}} \quad (1)$$

followed by the density log at the same depth (RHOB), neutron log (NPHI), and finally the sonic log (DT). And the output data,

Table 1. Number of samples on which Core were performed

Well	Effective porosity samples	Permeability samples
MAL-102	62	51
MAL-107	90	82
MAL-111	115	100

Table 2. Measurements available on the wells selected for the study

WELL		Open hole log							Core	
		CAL	GR	VCL	RT	RHOB	NPHI	DT	EFFECTIVE POROSITY	PERMEABILITY
Training wells	MAL-102	✓	✓	✓	✓	✓	✓	✓	✓	✓
	MAL-111	✓	✓	✓	✓	✓	✓	✓	✓	✓
Testing well	MAL-107	✓	✓	✓	✓	✓	✓	✓	✓	✓
generalization wells	MAL-103	✓	✓	✓	✓	✓	✓	✓	×	×
	MAL-115	✓	✓	✓	✓	✓	✓	✓	×	×

which includes measurements of permeability and effective porosity and serves as the target dataset for predicting permeability and effective porosity curves, was organized into another TXT file. The first column represents depth, the second column shows the effective porosity value (PHI), followed by the permeability measurement at the same depth (K), obtained from core analyses. A normalization process was conducted to constrain the input values within the range of 0 to 1. Tables 1, 2 and 3 presents a sample of the normalization process applied to the network's input and output.

3.3. Writing the code

The algorithm was developed to create a system that aligns with the problem at hand, allowing precise control over the neural network structure based on the available data and its size. The network's input consists of well logging parameters (CAL, VCL, NPHI, RHOB, DT), and the output represents the predicted permeability and effective porosity values. The LOGSIG activation function was applied to the layers of the neural network, with a learning rate of 0.05 and a momentum coefficient of 0.95. The

Table 3. Sample of network input and output data post and pre-normalization process.

post-normalization							pre-normalization						
LOGS					CORE		LOGS					CORE	
CAL IN	VCL %	RHOB G/C3	NPHI V/V	DT US/F	PHI %	K md	CAL IN	VCL %	RHOB G/C3	NPHI V/V	DT US/F	PHI %	K md
12.53	0.04	2.36	0.08	70.64	0.13	725	0.983	0.044	0.787	0.232	0.505	0.132	0.207
12.54	0.04	2.38	0.08	69.45	0.15	1560	0.983	0.045	0.794	0.230	0.496	0.145	0.446
12.50	0.11	2.41	0.09	67.64	0.19	770	0.981	0.106	0.804	0.239	0.483	0.185	0.220
12.51	0.18	2.40	0.10	66.76	0.14	260	0.981	0.182	0.799	0.249	0.477	0.140	0.074
12.58	0.06	2.35	0.10	67.81	0.13	499	0.987	0.061	0.785	0.253	0.484	0.131	0.143

minimum square error rate was set at 0.00001. A trainable sequential forward backpropagation algorithm (newcf) was used, suitable for solving complex and non-linear problems.

3.4. Structure of ANN

The network structure, including the number of hidden layers and neurons in each layer, was determined through empirical experimentation during the training of the neural network. Multiple configurations of neurons and hidden layers were tested to achieve the optimal structure, which provided the lowest error value within the training dataset (Table 4). Figure 4 illustrates the training dataset using the proposed neural network. The final network structure comprised three hidden layers: the first with 15 neurons, the second with 10 neurons, and the third with 4 neurons.

3.5. ANN performance train

To evaluate the performance of the neural network, the number of cycles it performed in search of the best solution was plotted against the mean square error values calculated during training to minimize error, as illustrated in Figure 5. The performance of the neural network, specifically in the section devoted to training, was assessed based on its ability to calculate permeability and effective porosity values that closely matched those obtained from core analyses. The network achieved its best performance at 12,000 cycles, where it completed its training.

The mean square error value neared 1, reflecting the robustness of the training process and highlighting the strong correlation between the actual data and the predicted values. This relationship is further demonstrated in Figure 6.

3.6. ANN performance test

In this stage, the performance of the ANN was tested using 35% of the data (MAL-107). This dataset included a set of borehole geophysical measurements and core analyses, which were selected to assess the ANN's performance in predicting permeability and effective porosity values (Figure 7).

Table 4. ANN optimized parameters (Ops).

Parameter	Tested	OPs
Neurons numbers	8-30	29
Hidden layers	1-3	3
Algorithm function	TANSIG / LOGSIG	LOGSIG
Learning rate	0.01-0.1	0.05

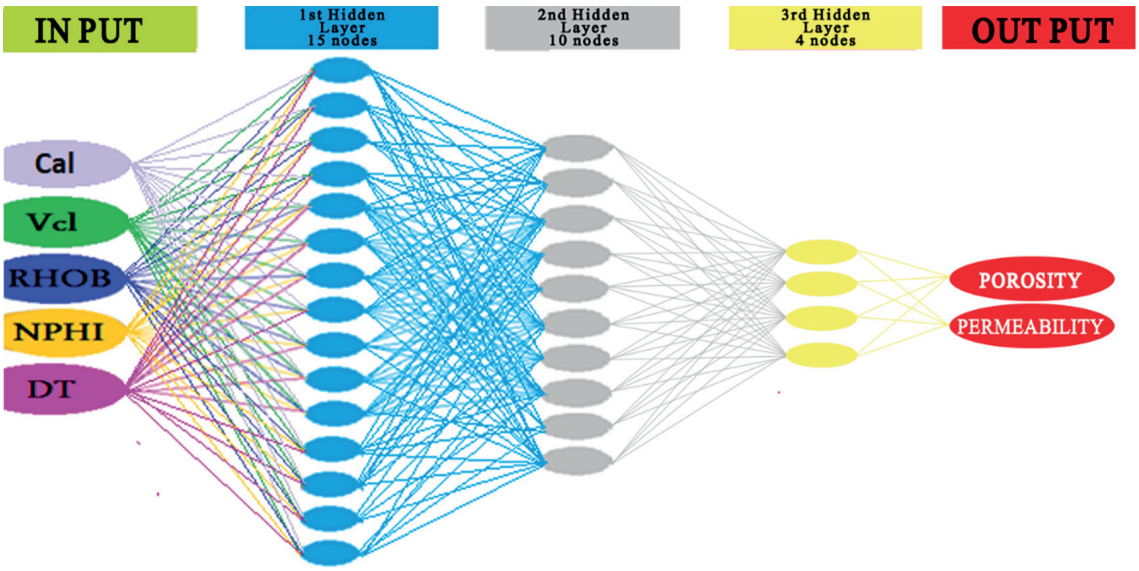

Figure 4. Structure of ANN used to predict permeability and effective porosity

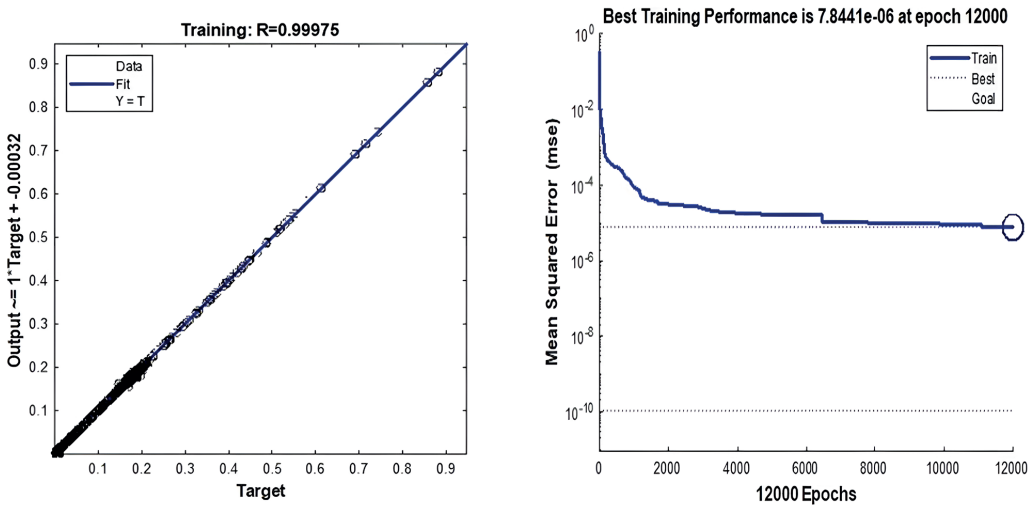

Figure 5. Performance of the neural network during training in the well.

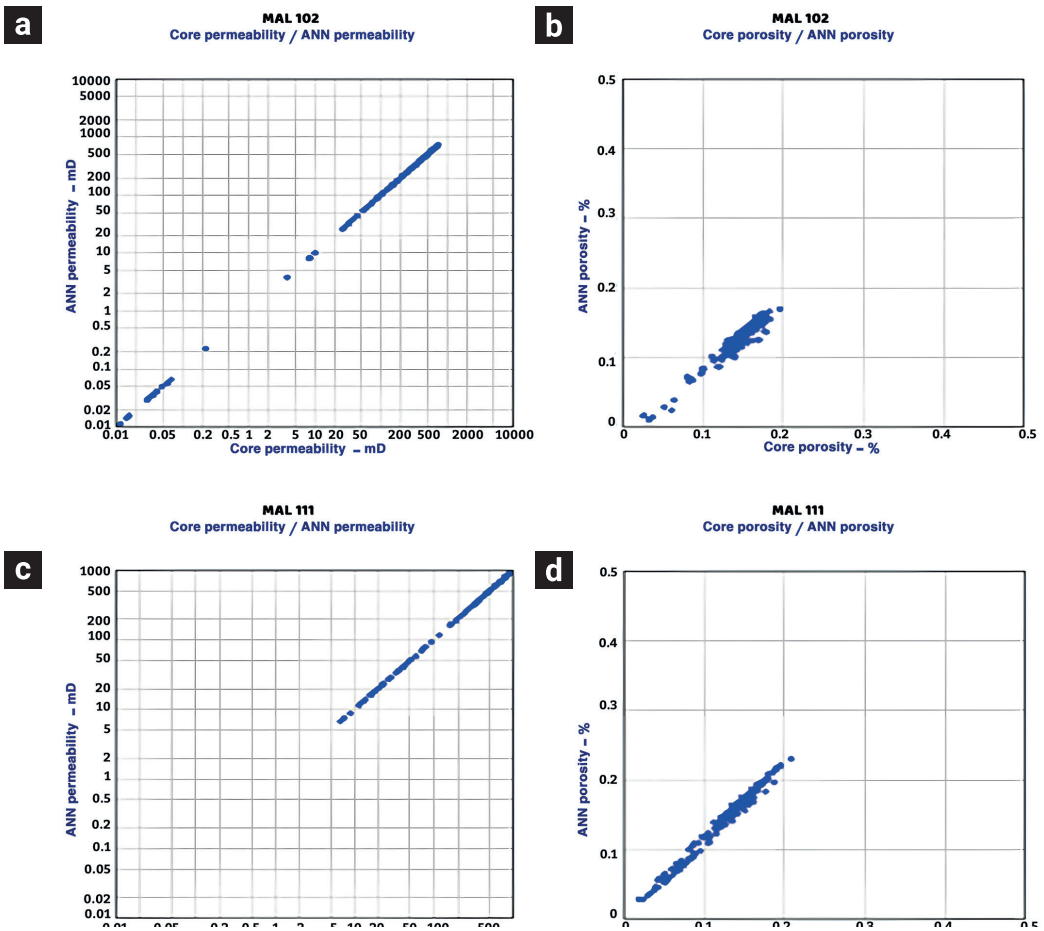

Figure 6. Relationship between core data and ANN-based predictions a) Analysis of the permeability correlation between core measurements and ANN predictions in well MAL 102. b) Analysis of the effective porosity correlation between core measurements and ANN predictions in well MAL 102. c) Analysis of the permeability correlation between core measurements and ANN predictions in well MAL 111. d) Analysis of the effective porosity correlation between core measurements and ANN predictions in well MAL 111.

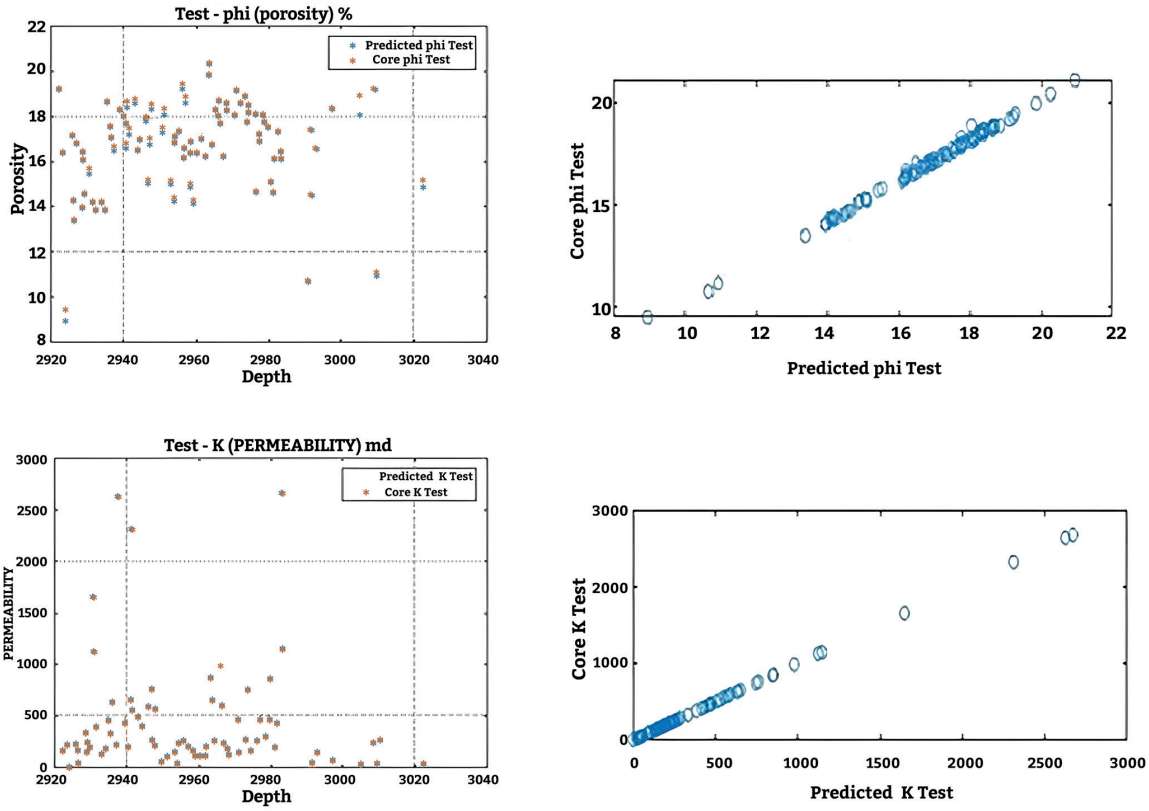

Figure 7. Testing the results of the ANN using the test data.

The accuracy of predicting effective porosity was about 96% and permeability was 97%, and this was illustrated in Figure 8.

The Kunzi-Carman equation was applied to compare its results with the results of the neural network, The generalized Kozeny-Karman model is a cornerstone in estimating the permeability of porous media, especially sandstones. Its effectiveness lies in its -ability to relate the physical properties of the rock, such as porosity and grain size, to the permeability. The generalized Kozeny-Carman equation can be expressed as follows:

$$K = \frac{1}{C \cdot S^2} \times \frac{\emptyset^3}{(1-\emptyset)^2} \quad (2)$$

K : permeability
∅ : porosity
S : Specific surface area per unit volume of particles
C : Kozeny constant (dimensionless)

The porosity was calculated based on the density log according to the following equation:

$$\emptyset = \frac{\rho_{ma} - \rho_{bulk}}{\rho_{ma} - \rho_{fluid}} \quad (3)$$

ρ_{ma} : Density of the rock matrix
ρ_{bulk} : Bulk density from the density log
ρ_{fluid} : Density of the pore fluid

The application of Equations 2 and 3 facilitated the calculation of permeability and porosity, with the results subsequently compared to core data. The analysis revealed that the predictions made by the neural network exhibited a stronger correlation and higher accuracy than the values computed for porosity and permeability, as illustrated in Figures 9 and 10.

The predicted permeability and effective porosity of the ANN and core sample for MAL 107 was represented (Figure 11) on the IP-2018 program.

3.7. generalizing the ANN

After testing the network, it was found that the accuracy in obtaining effective porosity and permeability values closely

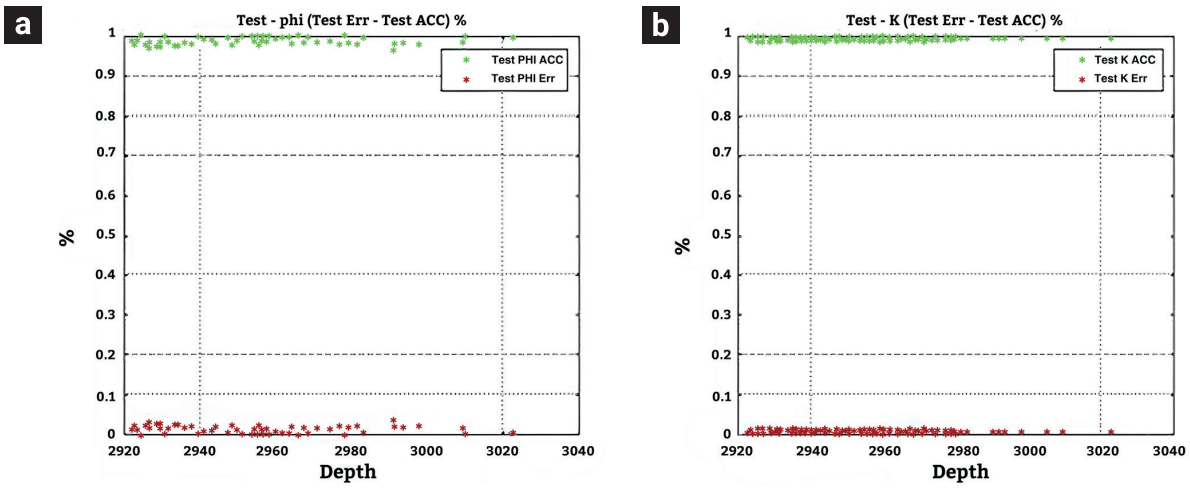

Figure 8. Accuracy and error percentage. a) Accuracy and error percentage for effective porosity. b) Accuracy and error percentage for permeability.

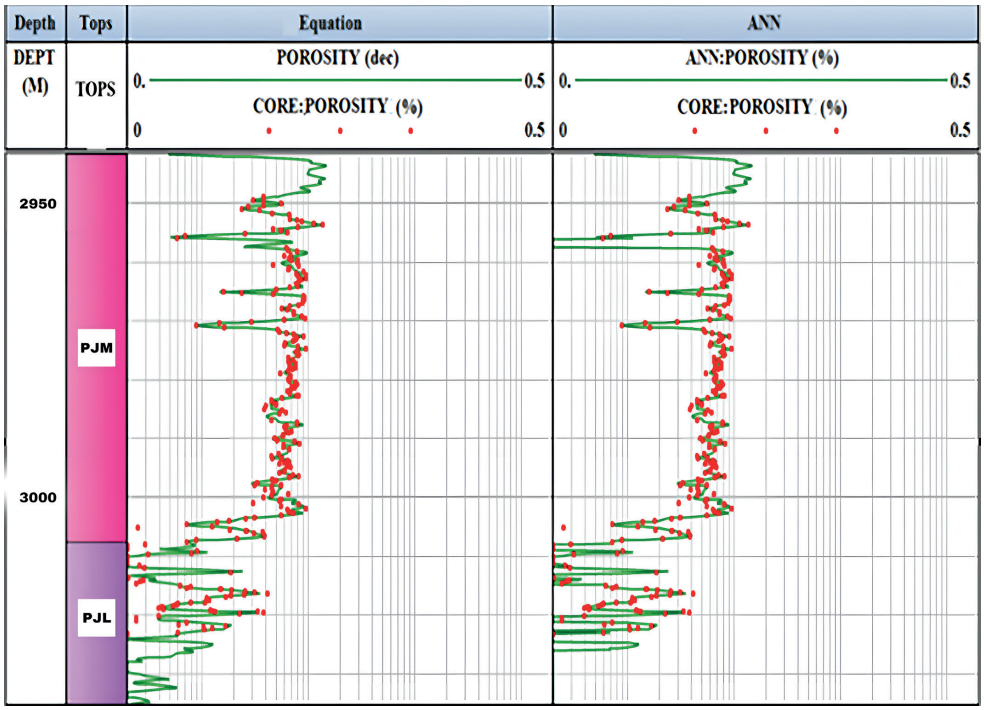

Figure 9. Comparison of porosity values calculated using empirical equations and those predicted by the ANN model for well MAL 107.

matched those derived from core samples. Wells MAL-103 and MAL-115, which did not have core samples, were selected for generalization.

These wells included all the well measurements used as network inputs. Consequently, the geophysical well measurements for these wells, covering the entire depth range of the PJS formation, were entered into the network. The network was then generalized to these wells, resulting in the predicted permeability and effective porosity curves. These results are illustrated using the IP-2018 software in Figures 12 and 13.

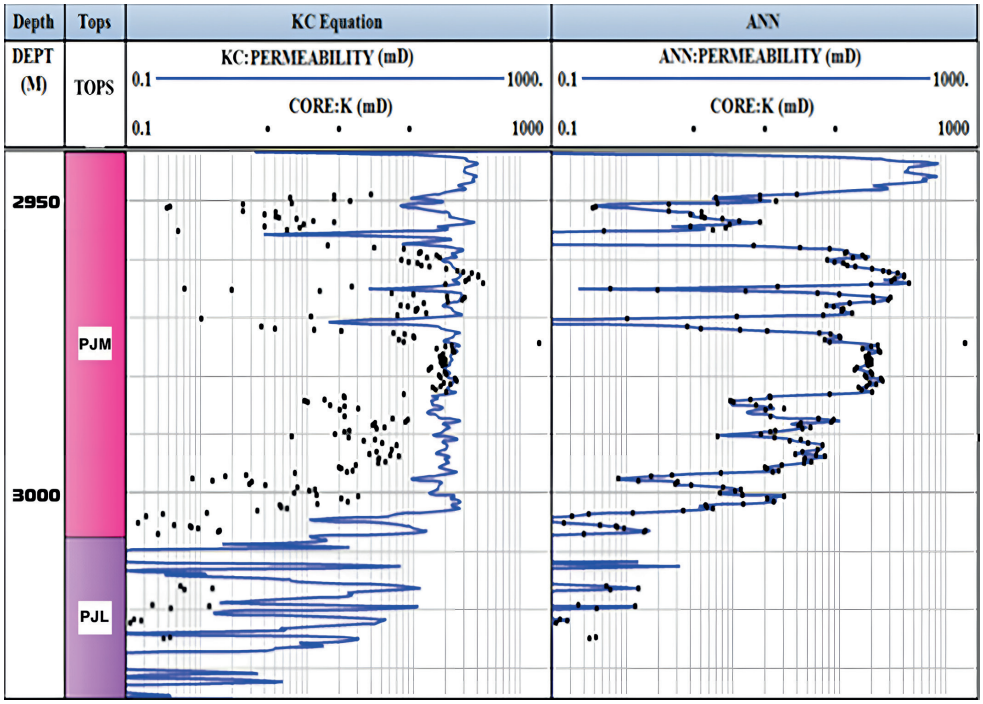

Figure 10. Comparison of permeability values calculated using the Kozeny-Karman equation and those predicted by the ANN model for well MAL 107.

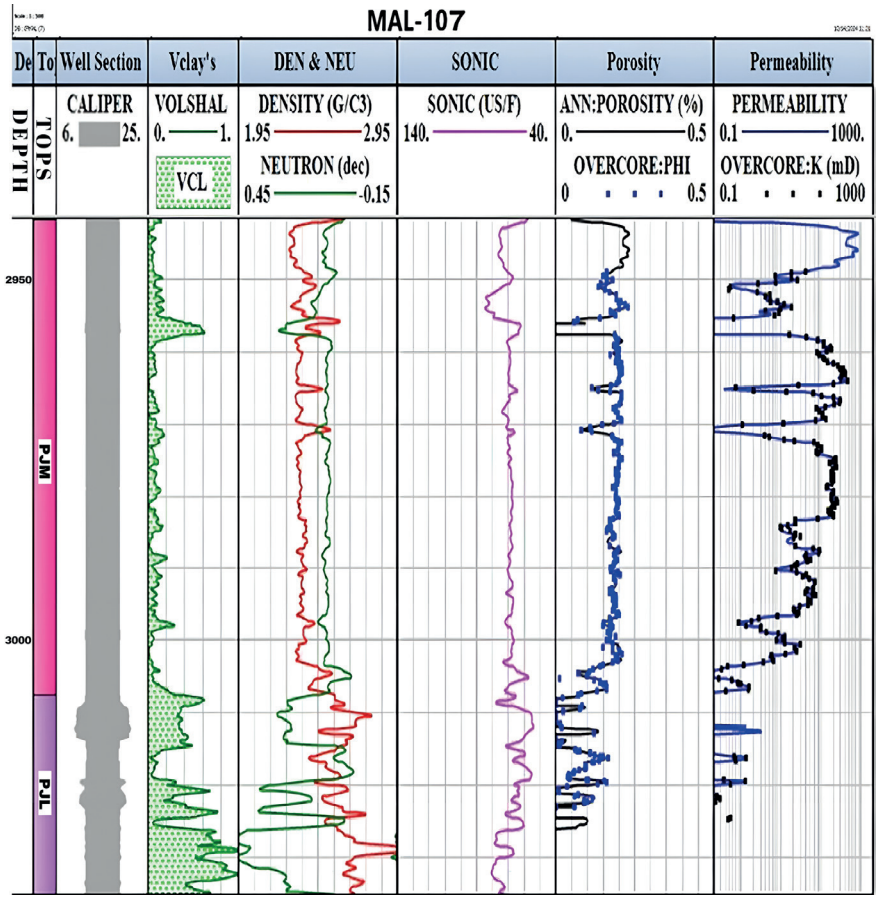

Figure 11. The well logs used as inputs for the ANN model and the resulting predictions of permeability and effective porosity for well MAL 107.

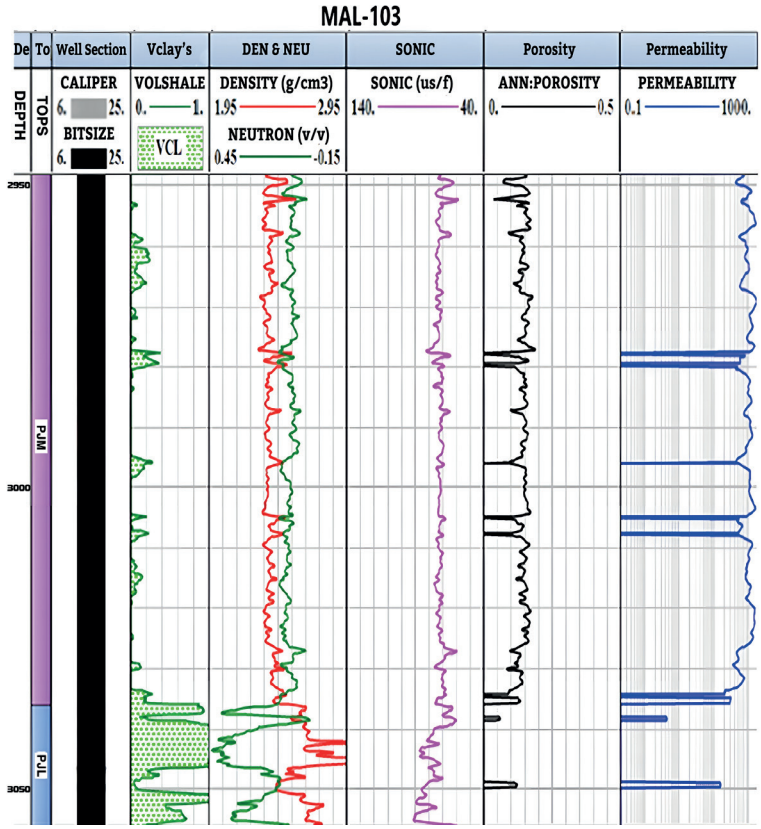

Figure 12. input of the ANN and the permeability and effective porosity values resulted by the ANN for the MAL-103.

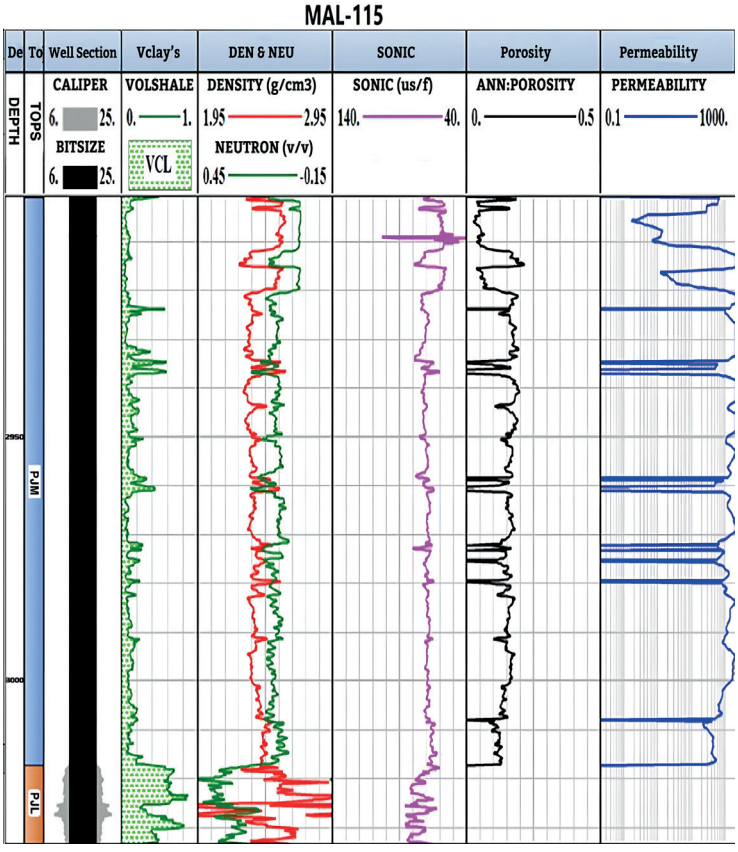

Figure 13. input of the ANN and the permeability and effective porosity values resulted by the ANN for the MAL-115 .

4. Results

The primary aim of this research was to estimate permeability and effective porosity values in wells where core samples were not available. Artificial neural networks were utilized, characterized by the simplicity of the mathematical relationships involved and their efficiency in processing data.

To achieve this, both the generalized Kozeny-Carman model and neural network methodologies were applied, offering a comparison between classical theoretical models and modern machine learning techniques in estimating the permeability of porous media, particularly sandstones. The Kozeny-Carman model adopts a physics-based approach, establishing deterministic relationships between rock properties such as porosity and grain size, while relying on the assumption of a well-defined pore structure. In contrast, neural networks utilize a data-driven approach, uncovering complex, nonlinear patterns in diverse datasets and adapting effectively to irregularities within the media.

Experimental testing and validation were conducted on the neural network architecture, where the best prediction results were achieved with a three-layer structure. The first layer contained 15 neurons, the second had 10, and the third included 4.

Through the application of these technologies, the research successfully predicted permeability and effective porosity with high precision, achieving approximately 96% accuracy for porosity prediction and 97% for permeability estimation. The high accuracy values in the neural network testing on well MAL-107 data were demonstrated using the Scatter and Residual Plots shown in Figure 14. These plots demonstrate the high predictive efficiency achieved by the proposed neural network.

This algorithm presents significant economic and practical advantages, enabling the accurate estimation of permeability

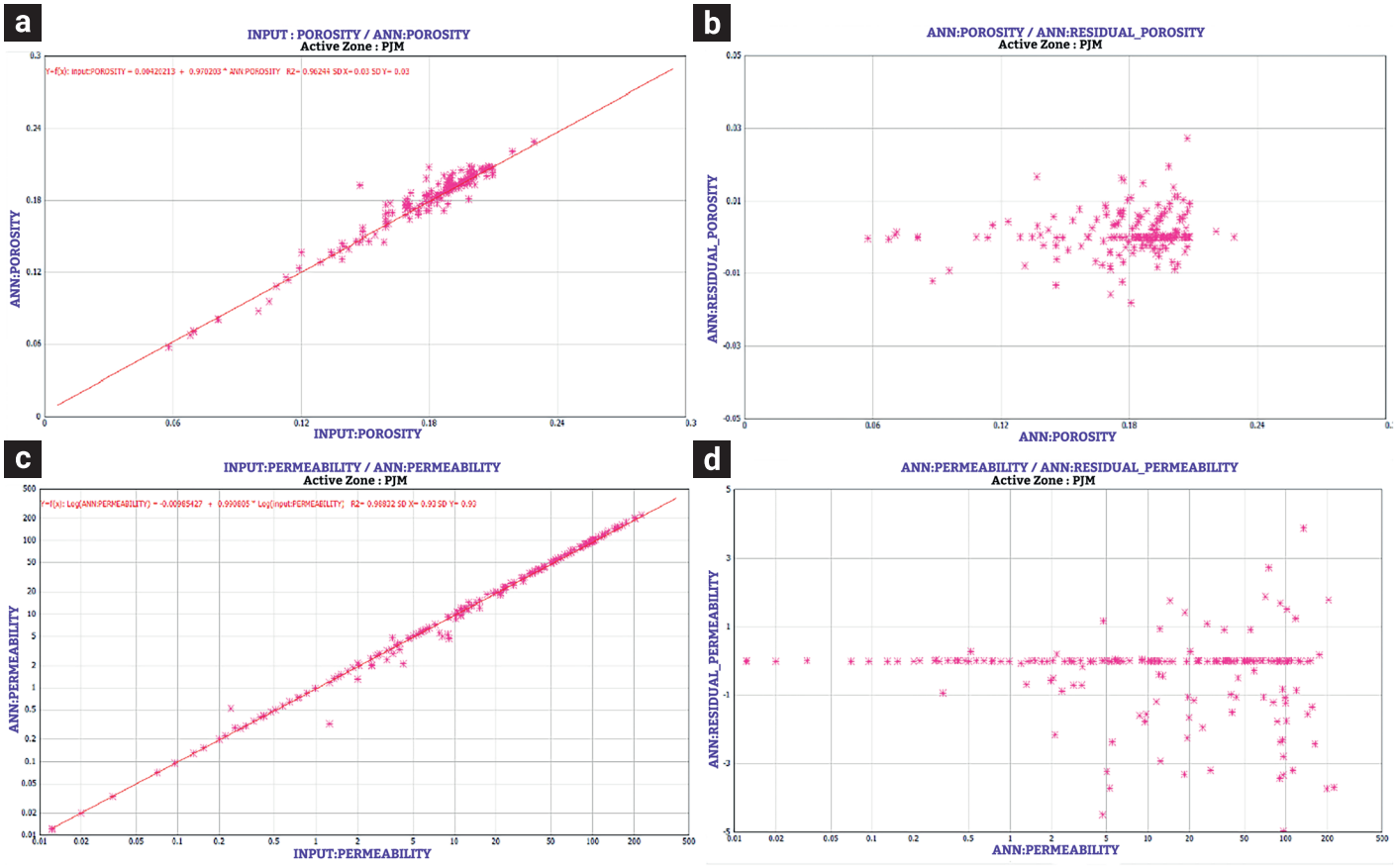

Figure 14. Scatter and Residual Plot of the ANN-based predictions. a) Scatter plot of the prediction effective porosity in well MAL 107. b) Residual Plot of the prediction effective porosity in well MAL 107. c) Scatter plot of the prediction permeability in well MAL 107. d) Residual Plot of the prediction permeability in well MAL 107.

and effective porosity in wells without the need for core samples or laboratory analyses. By streamlining the evaluation process, it not only enhances efficiency but also reduces time and costs associated with conventional methods. The ability to achieve reliable predictions with minimal resources underscores its potential as a transformative tool in reservoir characterization, paving the way for more data-driven and cost-effective approaches in subsurface studies.

5. References

Anifowose, F., Labadin, J., Abdulraheem, A. (2013). A least-square-driven functional networks type-2 fuzzy logic hybrid model for efficient petroleum reservoir properties prediction. Neural Computing and Applications, 23, 179–190. doi: **https://doi.org/10.1007/s00521-012-1298-2**

Chehrazi, A., Rezaee, R. A. (2012). A systematic method for permeability prediction, a Petro-Facies approach. Journal of Petroleum Science and Engineering, 82-83, 1–16. doi: **https://doi.org/10.1016/j.petrol.2011.12.004**

Chen, Y., Chang, H., Meng, J., Zhang, D. (2019). Ensemble Neural Networks (ENN): A gradient-free stochastic method. Neural Networks, 110, 170–185. doi: **https://doi.org/10.1016/j.neunet.2018.11.009**

De Ruiter, R. S. C., Lovelock, P. E. R., & Nabulsi, N. (1995). The Euphrates Graben of eastern Syria: A new petroleum province in the northern Middle East. In: Al-Husseini, M. I. (Ed.). GEO 94: The Middle East Petroleum Geosciences, 1. (pp. 357-36). Gulf PetroLink, Manama, Bahrain, 8.

Fadhil, D. T., Yonus, W. A., Theyab, M. A. (2020). Reservoir characteristics of the Miocene age formation at the Allas Dome, Hamrin Anticline, Northern Iraq. Mining of Mineral Deposits, 14(4), 17–23. doi: **https://doi.org/10.33271/mining14.04.017**

Helle, H. B., Bhatt, A. (2002). Fluid saturation from well logs using committee neural networks. Petroleum Geoscience, 8(2), 109–118. doi: **https://doi.org/10.1144/petgeo.8.2.109**

Khayer, K., Roshandel Kahoo, A., Soleimani Monfared, M., Tokhmechi, B., Kavousi, K. (2022). Target-Oriented Fusion of Attributes in Data Level for Salt Dome Geobody Delineation in Seismic Data. Nat. Resour, 31, 2461–2481. doi: **https://doi.org/10.1007/s11053-022-10086-z**

Lim, J. S., Kim, J. (2004). Reservoir porosity and permeability estimation from well logs using fuzzy logic and neural networks. [Presentación de paper]. SPE Asia Pacific Oil and Gas Conference and Exhibition, Perth, Australia. doi: **https://doi.org/10.2118/88476-MS**

Lis- Śledziona, A. (2019). Petrophysical rock typing and permeability prediction in tight sandstone reservoir. Acta Geophysica, 67, 1895–1911. doi: **https://doi.org/10.1007/s11600-019-00348-5**

Litak, R. K., Barazangi, M., Brew, G., Sawaf, T., Al-Imam, A., & Al-Youssef, W. (1998). Structure and Evolution of the Petroliferous Euphrates Graben System, Southeast Syria. AAPG Bulletin, 82(6), 1173–1190. doi: **https://doi.org/10.1306/1D9BCA2F-172D-11D7-8645000102C1865D**

Lu, H., Tang, H., Wang, M., Li, X., Zhang, L., Wang, Q., Zhao, Y., Zhao, F., Liao, J. (2021). Pore structure characteristics and permeability prediction model in a cretaceous carbonate reservoir, North Persian Gulf Basin. Geofluids, 8876679. doi: **https://doi.org/10.1155/2021/8876679**

Rezaee, R., Saeedi, A., Clennell, B. (2012). Tight gas sands permeability estimation from mercury injection capillary pressure and nuclear magnetic resonance data. Journal of Petroleum Science and Engineering, 88-89, 92–99. doi: **https://doi.org/10.1016/j.petrol.2011.12.014**

Smith, K. A. (1999). Neural networks for combinatorial optimization: A review of more than a decade of research. INFORMS Journal on Computing,11(1), 15–34. doi: **https://doi.org/10.1287/ijoc.11.1.15**

Sultan, M. Z. B. , Howladar, M. F. (2013). Permeability Modeling from well logs using artificial neural networks, Bangladesh. Mechanical Engineering Research Journal, 9, 100-103.

Zhang, D., Yuntian, C. H. E. N., Jin, M. E. N. G. (2018). Synthetic well logs generation via Recurrent Neural Networks. Petroleum Exploration and Development, 45(4), 629–639. doi: **https://doi.org/10.1016/S1876-3804(18)30068-5**

Zhong, Z., Carr, T. R., Wu, X., Wang, G. (2019). Application of a convolutional neural network in permeability prediction: A case study in the Jackson burg-Springtown oil field, West Virginia, USA. Geophysics, 84(4), 363–373. doi: **https://doi.org/10.1190/geo2018-0588.1**